



HAL
open science

Investigation of Action Pattern of a Novel Chondroitin Sulfate/Dermatan Sulfate 4- O -Endosulfatase

Wenshuang Wang, Cédric Przybylski, Xiaojuan Cai, Chrystel Lopin-Bon, Runmiao Jiao, Liran Shi, Kazuyuki Sugahara, José Neira, Régis Daniel, Fuchuan Li

► **To cite this version:**

Wenshuang Wang, Cédric Przybylski, Xiaojuan Cai, Chrystel Lopin-Bon, Runmiao Jiao, et al.. Investigation of Action Pattern of a Novel Chondroitin Sulfate/Dermatan Sulfate 4- O -Endosulfatase. *Biochemical Journal*, 2020, 478 (2), pp.281-298. 10.1042/BCJ20200657 . hal-03098070

HAL Id: hal-03098070

<https://univ-evry.hal.science/hal-03098070>

Submitted on 26 Nov 2021

HAL is a multi-disciplinary open access archive for the deposit and dissemination of scientific research documents, whether they are published or not. The documents may come from teaching and research institutions in France or abroad, or from public or private research centers.

L'archive ouverte pluridisciplinaire **HAL**, est destinée au dépôt et à la diffusion de documents scientifiques de niveau recherche, publiés ou non, émanant des établissements d'enseignement et de recherche français ou étrangers, des laboratoires publics ou privés.

Investigation of Action Pattern of a Novel Chondroitin Sulfate/Dermatan Sulfate 4-*O*-Endosulfatase

Wenshuang Wang¹, Cédric Przybylski^{2,3}, Xiaojuan Cai¹, Chrystel Lopin-Bon⁴, Runmiao Jiao¹, Liran Shi¹, Kazuyuki Sugahara⁵, José L. Neira⁶, Régis Daniel^{2*}, and Fuchuan Li^{1*}

¹National Glycoengineering Research Center and Shandong Provincial Key Laboratory of Carbohydrate Chemistry and Glycobiology, Shandong University, Qingdao 266237, P. R. China.

²Université Paris-Saclay, CNRS, Univ. Evry, Laboratoire Analyse et Modélisation pour la Biologie et l'Environnement, F-91025 Evry, France

³Sorbonne Université, CNRS, Institut Parisien de Chimie Moléculaire, IPCM, F-75005 Paris, France

⁴ICOA, CNRS UMR 7311, Université d'Orléans, F-45067 Orléans, France

⁵Department of Pathobiochemistry, Faculty of Pharmacy, Meijo University, Nagoya, Aichi 468-8503, Japan

⁶Instituto de Biología Molecular y Celular, Universidad Miguel Hernandez, Elche, Alicante, Spain

Correspondence

Fuchuan Li (fuchuanli@sdu.edu.cn) and Régis Daniel (regis.daniel@univ-evry.fr)

Abstract

Chondroitin sulfate (CS)/Dermatan sulfate (DS) sulfatases are potentially useful tools for exploring the structure-function relationship of CS/DS. Recently, a novel CS/DS 4-*O*-endosulfatase was identified from a marine bacterium and its catalytic mechanism was investigated further (Wang, W., et.al (2015) *J. Biol. Chem.* 290, 7823-7832; Wang, S., et.al (2019) *Front. Microbiol.* 10:1309). However, the effect of substrate structure on the activity of this enzyme remains to be studied. In this study, thirteen structure-defined hexasaccharides from CS polysaccharides were isolated and sequenced to investigate the specificities of this 4-*O*-endosulfatase. By using structure-defined CS oligosaccharides as substrates, we found that this 4-*O*-endosulfatase could effectively remove the 4-*O*-sulfate of disaccharide sequences GlcUA β 1-3GalNAc(4S) or GlcUA β 1-3GalNAc(4S,6S) in all tested hexasaccharides. However, it could not work on the 4-*O*-sulfate group of GlcUA β 1-3GalNAc(4S) connected to a disaccharide GlcUA(2S) β 1-3GalNAc(6S) in an octasaccharide, indicating the sulfation at C2 position of GlcUA might inhibited the action of this enzyme. Moreover, the 3-*O*-sulfation of D-glucuronic acid was also shown to inhibit the enzyme action. Additionally, the activity of this enzyme decreases with the increase of substrate size, and the saturation or not of the oligosaccharide substrates does not affect the specificity and action direction of the enzyme.

Introduction

Chondroitin sulfates (CS) / dermatan sulfates (DS) chains are composed of the repeating disaccharide (dp2) units with sulfate groups at various positions on the sugar residues (1). CS contains D-glucuronic acid (GlcUA) and N-acetyl-D-galactosamine (GalNAc), namely, -4GlcUA β 1-3-GalNAc β 1-. In DS where the GlcUA residues are epimerized into α -L-iduronic acid (IdoUA) by glucuronyl C-5 epimerase, the chains contain repeating disaccharide units of -4IdoUA α 1-3-GalNAc β 1- (1,2). Therefore, CS and DS often exist and periodically distribute in specific cell/tissue as a hybrid form (CS-DS) (3-5). Furthermore, CS/DS chains are modified by specific sulfotransferases in different positions (6), and sulfate groups can be mainly added to the C2 position of GlcUA/IdoA residues and the C4 and C6 positions of GalNAc residues. These modifications lead to several kinds of CS/DS disaccharide units including O/iO unit [GlcUA β 1-3GalNAc/ IdoUA α 1-3GalNAc], A/iA unit [GlcUA β 1-3GalNAc(4S)/IdoUA α 1-3GalNAc(4S)], B/iB unit [GlcUA(2S) β 1-3GalNAc(4S)/IdoUA(2S) α 1-3GalNAc(4S)], C/iC unit [GlcUA β 1-3GalNAc(6S)/IdoUA α 1-3GalNAc(6S)], D/iD unit [GlcUA(2S) β 1-3GalNAc(6S)/IdoUA(2S) α 1-3GalNAc(6S)], E/iE unit [GlcUA β 1-3GalNAc(4S,6S)/IdoUA α 1-3GalNAc(4S,6S)] and T/iT unit [GlcUA(2S) β 1-3GalNAc(4S,6S)/IdoUA(2S) α 1-3GalNAc(4S,6S)], where 2S, 4S and 6S represent 2-O-, 4-O- and 6-O-sulfate groups, respectively, and introduce enormous microheterogeneity within CS/DS chains. More and more studies have shown that various sulfation patterns gave different functions to CS/DS in biological processes (7-20) through interacting with various CS and/or DS-binding protein (21). Due to the structural complexity and diversity of CS/DS chains, it is a huge challenge for clarifying their structure-function relationships.

Sulfatases are a large enzyme family and can catalyze hydrolysis of sulfate esters in a wide range of substrates from small steroids to complex carbohydrates on cell surface, such as glycosaminoglycans (GAGs) (22). Increasing evidences show that sulfatases with different desulfation activities on specific sulfate esters of CS/DS chains are suitable and important tools for exploring the roles of CS/DS in various biological processes (23). CS/DS sulfatases are characterized by the desulfation of CS/DS saccharides and can be generally designated based on the desulfated position. For example, GalNAc-4-O-sulfatase and GalNAc-6-O-sulfatase catalyze the hydrolysis of the sulfate ester at the C4 and C6 position of GalNAc residues, respectively, and $\Delta^{4,5}$ HexUA-2-O-sulfatase hydrolyzes the sulfate ester on C2 position of the unsaturated hexuronate at the non-reducing end of CS/DS or heparin/heparan sulfate oligosaccharides generated by GAGs lyases (24-26). It is worth noting that most of the identified GAG sulfatases are exosulfatases, which attacks only the sulfate groups of saccharide residues at the end of GAG chains, in particular of short oligosaccharides from the digestion of GAGs by GAG-degrading enzymes (21,26). By contrast, only two CS/DS endosulfatases, which catalyze sulfate hydrolysis within the GAGs chains, have been reported so far. They have been individually identified in *Bacteroides thetaiotaomicron* (27) and *Vibrio* sp. FC509 (28), and both are 4-O-endosulfatase. Compared to exosulfatase, endosulfatases are more potent tools for structure-function-studies of CS/DS, but their action patterns remain to be characterized in detail.

In our previous study, the 4-O-endosulfatase from *Vibrio* sp. FC509 could efficiently remove the 4-O-sulfate from various CS/DS polysaccharides, with an efficiency of 17-65%. In the study herein, we

investigated whether structural determinants in the CS/DS polysaccharides may block the action of the endosulfatase, explaining why 4-*O*-sulfate groups were not fully removed in these polysaccharides. For that purpose, we have used a series of structure-homogenous hexasaccharides (dp6s) either from synthetic source or prepared from the polysaccharide substrates CS-A and CS-E and sequenced through an enzymatic method (29). By using these aforementioned hexasaccharides with other reported CS oligosaccharides as substrates, some important action features of the 4-*O*-endosulfatase were revealed. These delineated characteristic features will be very helpful for the application of this enzyme in the structural and functional studies of CS/DS.

Experimental Procedures

Materials

Standard CS unsaturated disaccharides were purchased from Iduron (Manchester, UK). CS-E from squid cartilage was obtained from Seikagaku Corp. (Tokyo, Japan). 2-aminobenzamide (2-AB), sodium cyanoborohydride (NaBH₃CN), CS-A from bovine trachea and CSase ABC (EC 4.2.2.4) were obtained from Sigma. The GAG endo-lyase (HCLase) (30), exo-lyase (HCDLase) (28) and CS/DS 4-*O*-endosulfatase (29) from a marine bacterium *Vibrio* sp. FC509 were obtained from our laboratory. CS-A or CS-E dp6s were prepared by digesting CS-A or CS-E using HCLase followed by gel filtration chromatography and anion exchange chromatography as described previously (30). Octasaccharide $\Delta^{4,5}\text{HexUA}\alpha 1\text{-3GalNAc}(6\text{S})\beta 1\text{-4GlcUA}\beta 1\text{-3GalNAc}(4\text{S})\beta 1\text{-4GlcUA}(2\text{S})\beta 1\text{-3GalNAc}(6\text{S})\beta 1\text{-4GlcUA}\beta 1\text{-3GalNAc}(6\text{S})$ ($\Delta\text{C-A-D-C}$) from Prof. Sugahara's Lab (31). Synthetic saturated di-, tetra- and hexasaccharides (dp2, dp4 and dp6) of CS-A (A, A-A and A-A-A) and various saturated dp2s GlcUA β 1-3GalNAc(6S) (C unit), GlcUA(2S) β 1-3GalNAc(6S) (D unit), GlcUA β 1-3GalNAc(4,6S) (E unit), GlcUA(3S) β 1-3GalNAc(4S) (K unit), GlcUA(3S) β 1-3GalNAc(6S) (L unit) and GlcUA(3S) β 1-3GalNAc(4,6S) (M unit) were prepared as previously described (32). All other chemicals and reagents were of the highest quality available.

Preparation of structure-homogenous CS dps

A commercial preparation (200 mg) of CS-A and CS-E was degraded by 0.1 U HCLase in 2.0 ml 50 mM Na₂HPO₄-NaH₂PO₄ buffer pH 6.5. The incubation proceeded at 35°C for 2 h. The reaction mixture was heated in boiling water for 10 min to stop the reaction and subsequently cooled in ice-cold water for 10 min. After being centrifuged at 15,000 × g for 15 min, the supernatant was collected and analyzed by gel filtration chromatography on a SuperdexTM Peptide 10/300 GL column (GE healthcare). The mobile phase was 0.2 M NH₄HCO₃ at a flow rate of 0.4 ml/min, and the eluted fractions were monitored at 232 nm (33) using a UV detector. Online monitoring and data analysis (e.g. molar ratio determination) were performed using the software LC solution version 1.25. The dp6 fraction of CS-A was subfractionated by anion exchange HPLC on a YMC-Pack Polyamine column (YMC, Kyoto, Japan) eluted with a linear gradient from 150 to 450 mM NaH₂PO₄ over 60 min at a flow rate of 1.0 ml/min (34). The dp6 of CS-E was subfractionated by anion exchange HPLC on a YMC-Pack Polyamine II column eluted with a linear gradient from 300 to 600 mM NaH₂PO₄ over 60 min at a flow rate of 1.0 ml/min. Then the subfractions of dp6s were repurified by anion exchange chromatography on a YMC-Pack PA-G column (YMC, Kyoto, Japan) under the same conditions. Separated fractions were desalted by gel filtration on SuperdexTM Peptide 10/300 GL column as described, and freeze-dried repeatedly to remove NH₄HCO₃ for further

identification.

The dp6 fractions (30 pmol) were labeled with 2-AB and sodium cyanoborohydride reagent as described by Bigge et al (35). Free 2-AB was removed by extraction with chloroform. An aliquot (5 pmol) 2-AB-labeled dp6s of CS-A were individually analyzed by anion-exchange HPLC on a YMC-Pack PA-G column eluted with a linear gradient from 16 to 460 mM NaH₂PO₄ over 60 min at a flow rate of 1.0 ml/min at room temperature, and an aliquot (5 pmol) 2-AB-labeled dp6s of CS-E were individually analyzed by anion-exchange HPLC on a YMC-Pack PA-G column eluted with a linear gradient from 16 to 690 mM NaH₂PO₄ over 90 min. The samples were monitored using a fluorescence detector with excitation and emission wavelengths of 330 and 420 nm, respectively.

Determination of the desulfated products of 4-*O*-endosulfatase by mass spectrometry

Desulfation of synthetic CS oligosaccharides by 4-*O*-endosulfatase was carried out as previously described (28). Briefly, 10 μ l of the enzyme preparation was mixed with 5 μ L of CS oligosaccharides (100 μ M final) in 35 μ L of 72 mM phosphate buffer, pH 8.1 (50 mM final), and incubated at 30 °C, for 1, 2, 3, 4, 5, 6 and 24 h. After incubation, the resulting oligosaccharides were isolated and desalted using a C18 + Carbon-SPE TopTip cartridge (Glygen, Columbia, MD, USA) as previously described (36). Each elution fraction was pooled, freeze-dried, and dissolved in 10 μ l water for MS analysis. MALDI-time-of-flight (TOF) mass spectrometer (MS) experiments were performed using a PerSeptive Biosystems Voyager-DE Pro STR mass spectrometer (Applied Biosystems/MDS SCIEX, Foster City, CA, USA) equipped with a nitrogen UV laser (337 nm wavelength) pulsed at 20 Hz frequency. The MS was operated in the negative ion reflector mode with an accelerating potential of -20 kV and a grid percentage equal to 70%. Mass spectra were recorded with the laser intensity set just above the ionization threshold (2900-3000 in arbitrary units, on our instrument) with a pulse width of 3 ns. An ion extraction delay was set to 150 and 300 ns for analyze with dp2, dp4 and dp6, respectively. Typically, mass spectra were obtained by accumulation of 100–200 laser shots for each analysis and processed using Data Explorer 4.0 software (Applied Biosystems). The HABA/TMG₂ ionic liquid, used as the matrix, was prepared by following a literature procedure (37).

Nano-electrospray (ESI)-MS and MS_n of CS oligosaccharides were carried out using a static probe coupled to LTQ-Orbitrap XL from Thermo Scientific (San Jose, CA, USA) and operated in negative ionization mode, with a spray voltage at -0.8 to -1.0 kV. Two microliters of each aqueous sample was continuously infused through a fused silica tip with a 360- μ m outer diameter, 20 μ m inner diameter with a nominal tip end inner diameter of 10 \pm 1.0 μ m (Pico-tip, FS360-50-15-CE-20-C10.5, New Objective, Woburn, MA, USA) which provided a consistent signal during 15 min. Applied voltages were -35 and -113 V for the ion transfer capillary and the tube lens, respectively. The ion transfer capillary was held at 200°C. Resolution was set to 30,000 (at m/z 400) for all studies, and the m/z ranges were set to 150-2000 in profile mode and in the normal mass range. Spectra were analyzed using the acquisition software XCalibur 2.0.7 (Thermo Scientific, San Jose, CA, USA), without smoothing or background subtracts. During MS/MS scans, collision-induced dissociation (CID) fragmentation occurred in the linear ion-trap analyzer and detection in Orbitrap with centroid mode. For CID fragmentation, an activation Q value of 0.25 and an activation time equal to 30 ms were used. Normalized collision energy (NCE) was set at 25% for MS₂/MS experiments and 15-25% for MS_n experiments (with n>2). The automatic gain control (AGC) allowed accumulation up to 1.10⁶ ions for Fourier-transform MS (FTMS) scans, 2.10⁵ ions for

FTMSn scans and 1.10^4 ions for ion-trap MS (ITMSn) scans. Maximum injection time was set to 500 ms for both FTMS and FTMSn scans and 100 ms for ITMSn scans. For all scan modes, 1 μ s scan was acquired. The precursor selection window was 2 Da and 3 Da during MS² and MSn (with $n > 2$), respectively. Each ion with $z \geq 2$ present in the full-scan MS and exhibiting a signal intensity of >500 arbitrary units was fragmented by iterative ESI-MSn steps (with $n \geq 2$). Fragments resulting from fragmentation steps were annotated according to the nomenclature described by Domon and Costello (38).

Sequencing of CS structure-homogenous dp6s

Firstly, the disaccharide composition of each CS dp6 (5 pmol) was determined by complete digestion with 5 mU CSase ABC and labeled by 2-AB followed by anion exchange HPLC (35). Then, the disaccharide at the non-reducing end of each CS dp6 was determined by digestion of 2-AB-labeled dp6 with CSase ABC and relabeling with 2-AB followed by analysis with anion exchange HPLC (28). Briefly, an aliquot (5 pmol) of 2-AB-labeled dp6 were degraded with 5 mU CSase ABC, and then the digest was relabeled with 2-AB. After removing free 2-AB by extraction with chloroform, the resulted sample was analyzed by anion exchange HPLC. Finally, the disaccharide located at the reducing end of dp6 was identified by digestion of 2-AB-labeled dp6 with HCDLase, because this enzyme is a novel exolyase that can remove 2-AB labeled sulfated but not unsulfated disaccharides from the reducing ends of 2-AB-labeled CS oligosaccharides (29). All these preparations were individually analyzed by anion-exchange HPLC on a YMC-Pack PA-G column eluted with a linear gradient from 16 to 460 mM NaH₂PO₄ over 60 min at a flow rate of 1.0 ml/min at room temperature, and the samples were monitored using a fluorescence detector with excitation and emission wavelengths of 330 and 420 nm, respectively (39). Identification and quantification of the resulting disaccharide units were achieved by comparison with CS-derived authentic unsaturated disaccharide units (40).

Substrate-degrading characteristic analysis of 4-O-endosulfatase

An aliquot (10 pmol) of CS dp6 and dp8 fractions were treated with 20 mU 4-O-endosulfatase in 50 mM NaH₂PO₄-Na₂HPO₄, pH 8.0, at 30°C for 72 h, respectively (28). Enzyme-treated products were heated in boiling water for 10 min and then cooled in ice-cold water for 10 min. After centrifugation at 15,000 \times g for 15 min, the supernatants were collected. Half amounts of the samples were further degraded with 5 mU CSase ABC for disaccharide composition determination. Then all samples were labeled by 2-AB and individually analyzed by anion exchange HPLC on a YMC-Pack PA-G column at a flow rate of 1.0 ml/min at room temperature. The resultants of CS-A dp6, CS-E dp6 and dp8 Δ C-A-D-C treated with 4-O-endosulfatase were eluted with a linear gradient from 16 to 460 mM NaH₂PO₄ over 60 min, from 16 to 690 mM NaH₂PO₄ over 90 min and from 300 to 800 mM NaH₂PO₄ over 60 min, respectively. Disaccharide composition analysis of these dp6 and dp8 samples treated with or without 4-O-endosulfatase was carried out by anion exchange HPLC on a YMC-Pack PA-G column eluted with a linear gradient from 16 to 460 mM NaH₂PO₄ over 60 min. And all the samples were monitored using a fluorescence detector with excitation and emission wavelengths of 330 and 420 nm, respectively. To illustrate the effect of the CS-A length on the activity of the 4-O-sulfatase, size-defined CS-A oligosaccharides (1 μ g) with different lengths were treated with 4-O-endosulfatase (1 mU) for 10 min, and then the disaccharide composition of each reaction was analyzed as described above.

Results

Isolation of CS unsaturated dp6s

A commercial preparation (200 mg) of CS-A and CS-E were partially digested with 0.1 U endolyase HCLase, and the resulting oligosaccharides were fractionated by a Superdex™ Peptide 10/300 GL column (Figure S1). Then dp6s from CS-A (Figure S2A) and CS-E (Figure S2B) were subfractionated by HPLC on anion exchange column of YMC-Pack Polyamine II and YMC-Pack PA-G, respectively. Thirteen main dp6 fractions were obtained. Purified dp6s were labeled by 2-AB and analyzed by fluorescent HPLC for purity. Each purified fraction gave a single symmetrical peak, confirming its high purity. All thirteen pure dp6s fractions were obtained for further sequencing and the desulfation pattern studies of 4-*O*-endosulfatase.

Sequencing of purified CS dp6 preparations

To determine the sequences of the dp6s prepared from CS-A and CS-E, the disaccharide composition and disaccharides located at the non-reducing and reducing end of each dp6 were determined by an enzymatic method (29). For disaccharide composition analysis, dp6 fractions were individually digested by CSase ABC, labeled by 2-AB, and then analyzed by anion-exchange HPLC. Fractions CS-A7 and CS-A11 yielded a single disaccharide specie, $\Delta^{4,5}\text{HexUA}\alpha\text{1-3GalNAc(6S)}$ (ΔC unit) (Figure 1D and Table 1), and $\Delta^{4,5}\text{HexUA}\alpha\text{1-3GalNAc(4S)}$ (ΔA unit), respectively, and the peak of the resulted disaccharide was about 3-fold higher than that of its parental dp6 (Figure 1 and Table 1). Therefore, the sequences of CS-A7 and CS-A11 must be $\Delta\text{C-C-C}$ and $\Delta\text{A-A-A}$ (Table 2), respectively. The disaccharide composition of other nine dp6 fractions showed that all of them contain two different disaccharide units: ΔA unit and $\Delta^{4,5}\text{HexUA}\alpha\text{1-3GalNAc}$ (ΔO unit) for CS-A4 (Figure 1B and Table 1) and CS-A5 (Figure 1C and Table 1), ΔC unit and ΔA unit for CS-A9 (Figure 1E and Table 1), CS-A10-2 (Figure 1G and Table 1), CS-A10-3 (Figure 1H and Table 1), and for CS-A10-1 (Figure 1F and Table 1), ΔA unit and $\Delta^{4,5}\text{HexUA}\alpha\text{1-3GalNAc(4S,6S)}$ (ΔE unit) for CS-E9 (Figure 1K and Table 1) and for CS-E15 (Figure 1M and Table 1), ΔC unit and ΔE unit for CS-E13 (Figure 1L and Table 1) in a molar ratio of 2:1. Digestion of CS-A3 or CS-E7 by CSase ABC yielded three different disaccharide units: ΔO unit, ΔC unit and ΔA unit of CS-A3 (Figure 1A and Table 1), or ΔC unit, ΔA unit and ΔE unit of CS-E7 (Figure 1J and Table 1) in a molar ratio of 1:1:1.

To determine the disaccharide units from the non-reducing terminus, 2-AB-labeled non-sequenced dp6 fractions (Figure S3) were digested by CSase ABC and relabeled with 2-AB for HPLC analysis (28). The amount of two products, the non-reducing end disaccharide and reducing end tetrasaccharide of parental dp6, were equal and 1.0-fold of the substrate oligosaccharide approximately, respectively, which further indicated that all the oligosaccharides isolated from CS-A and CS-E were dp6 (Figure S3). The disaccharide units from non-reducing ends were ΔO unit for CS-A4 (Figure S3B), ΔC unit for CS-A3 (Figure S3A), CS-A10-2 (Figure S3F) and CS-A10-3 (Figure S3G), ΔA unit for CS-A5 (Figure S3C), CS-A9 (Figure S3D) and CS-A10-1 (Figure S3E), and ΔE unit for CS-E7 (Figure S3H), CS-E9 (Figure S3I), CS-E13 (Figure S3J) and CS-E15 (Figure S3K), respectively. At this point, the sequences of fractions CS-A4, CS-A9 and CS-E9 can be concluded according the disaccharide composition and disaccharide unit at non-reducing ends. The sequences of the fractions CS-A4, CS-A9 and CS-E9 are

Δ O-A-A, Δ A-C-C and Δ E-A-A, respectively (Table 2).

To identify the disaccharide units at the reducing ends of remained non-sequenced dp6 fractions, the 2-AB-labeled non-sequenced dp6 samples were further degraded with HCDLase followed by HPLC analysis using a fluorescence detector. As shown in Figure S4, CS-A3 and CS-A5 partially degraded by HCDLase due to the resistant of the middle O unit in the 2-AB-labeled dp6 to the digestion by HCDLase (29), and thus the released Δ A unit at the reducing end and its undigested parental dp6 were appeared together. Consequently, the sequences of CS-A3 and CS-A5 can be inferred as Δ C-O-A, Δ A-O-A, respectively. The disaccharide units from reducing ends of other dp6 were Δ C unit of CS-A10-1, CS-A10-2, CS-E7 and CS-E13 (Figure S4C, S4D, S4F and S4G), and Δ A unit of CS-A10-3 and CS-E15 (Figure S4E and S4H), respectively. Therefore, based on the results above, we can deduce that the structures of CS-A10-1, CS-A10-2, CS-A10-3, CS-E7, CS-E13 and CS-E15 were Δ A-A-C, Δ C-A-C, Δ C-C-A, Δ E-A-C, Δ E-E-C and Δ E-E-A, respectively (Table 2).

Influence of neighbour disaccharides on the digestion pattern by 4-*O*-endosulfatase

To investigate the digestion specificity of the 4-*O*-endosulfatase, thirteen structure-defined CS unsaturated dp6 with different sulfation patterns and a CS dp8 Δ C-A-D-C (31) were individually treated with 4-*O*-endosulfatase exhaustively. The reaction mixtures were directly analyzed by anion exchange HPLC to detect desulfated oligosaccharides. As shown in Figure 2, all samples except CS-A7 and Δ C-A-D-C were eluted at lower salt concentration than their corresponding parental oligosaccharides, suggesting that some sulfate groups were removed from these oligosaccharides.

To further identify the positions of the sulfate groups hydrolyzed by 4-*O*-endosulfatase, the enzyme-treated oligosaccharides were degraded with CSase ABC and then labeled with 2-AB for disaccharide composition analysis by anion exchange HPLC as described under “Experimental Procedures”. As shown in Figure 3 and Table 3, all the A and E units in dp6 oligosaccharides were transformed into the unsulfated disaccharide O units and monosulfated disaccharide C units, respectively. Based on the structures of all the test dp6 oligosaccharides, we can conclude that this 4-*O*-endosulfatase can completely remove the 4-*O*-sulfate group of A unit or E unit no matter they are at the reducing end, non-reducing end, or internal of dp6, and this desulfation of A unit or E unit in dp6 does not be inhibited by their adjacent O unit or C unit. However, when the dp8 Δ C-A-D-C was treated with 4-*O*-endosulfatase, the 4-*O*-sulfate group of A unit could not be removed (Figure 3 and Table 3), suggesting that the HexUA(2S)1-3GalNAc(6S) unit connected to A unit might inhibit the action of 4-*O*-endosulfatase.

Effect of substrate size on the activity of 4-*O*-endosulfatase

Although the optimal substrate CS-A is composed of major component A units and minor component O and C units, only 65% of A units were desulfated by the 4-*O*-endosulfatase even under a very strong reaction condition (28). We suppose that the enzymatic activity may be affected by the size of substrate. To investigate this hypothesis, the hydrolysis capacity of the endosulfatase on oligosaccharides saturated A of increasing size (dp2), A-A (dp4) and A-A-A (dp6) was determined by MALDI-TOF mass spectrometry at various incubation times. Under limited enzymatic activity the kinetics analysis showed a rapid and total decrease of intact A-A and A-A-A, indicating that the enzyme is able do catalyze the desulfation of these longer substrate molecules in few hours (Figure S5A). The initial decrease of the totally 4-*O*-sulfated species was faster with dp6, then dp4 and dp2, suggesting that the first 4-*O*-sulfate group on the longer substrate is easier to be removed. However, the total desulfation of A-A or A-A-A is much more time-consuming than that of A unit, indicating that chain length of

substrates affects the enzymatic activity (Figure. S5B). Then, the removal percentage of 4-*O*-sulfates from substrates with different length were analyzed by using a series of unsaturated CS-A oligosaccharides from dp2 to dp12 as substrates digested with 4-*O*-endosulfatase within a certain time (10 min). As shown in Table 4, the 4-*O*-desulfation ratio of A units in the prepared oligosaccharides were significantly decreased with the length increase of oligosaccharide substrates, thus explaining why the desulfation of CS-A polysaccharides by this 4-*O*-endosulfatase is relatively inefficient and incomplete.

Effect of saturated CS disaccharides on the action of 4-*O*-endosulfatase

In previous studies, the specificity and action pattern of the 4-*O*-endosulfatase were investigated on substrates with limited structural diversity by using common unsaturated CS oligosaccharides produced by CS/DS lyases (23). Here, the action of 4-*O*-endosulfatase was studied by using as substrate a larger library of synthetic CS based-saturated disaccharides including monosulfated A unit and C unit, disulfated E unit, D unit, K unit and L unit, and trisulfated M unit. MALDI-TOF MS analysis of the enzyme reaction products show that saturated A unit and E unit can be completely converted to O unit (m/z 396.11) and C unit (m/z 498.05), respectively, by the treatment with this endosulfatase (Figure S6), indicating that this enzyme shows the same specific activity of 4-*O*-desulfation whether the substrates are saturated or unsaturated (23). However, the 4-*O*-sulfates of K unit (GlcUA(3S) β 1-3GalNAc(4S)), L unit (GlcUA(3S) β 1-3GalNAc(6S)) and M unit (GlcUA(3S) β 1-3GalNAc(4,6S)) could not be removed, which may be due to the steric hindrance caused by the 3-*O*-sulfate of GlcUA to inhibit the activity of the endosulfatase (Figure S7).

Action pattern of the 4-*O*-endosulfatase on saturated CS oligosaccharide

In previous studies, we have shown that 4-*O*-endosulfatase can remove 4-*O*-sulfate groups starting from the reducing end to the non-reducing end of an unsaturated dp6 Δ A-A-A (41). To further investigate if the unique unsaturated uronic acid produced by the cleavage of CS/DS lyases is a key factor to affect the action direction of the endosulfatase, the desulfated products formed from a synthetic saturated dp6 A-A-A at various times of incubation with this enzyme have been sequenced by multistage mass spectrometry. The MS spectrum showed a major species at m/z 689.5937 after 3 h incubation, which corresponded to a disulfated dp6 product. The serial fragmentations from MS² to MS⁵ of this disulfated product indicated that the desulfated position was on the reducing end residue GalNAc (Figure 4A-D). In details, MS² of the doubly charged ion at m/z 689.5937 yielded a major C₅²⁻ ion at m/z 588.0510 corresponding to a disulfated pentasaccharide. It resulted from a glycosidic rupture releasing the terminal GalNAc unit at the reducing end of the parent dp6, thereby forming the C₅²⁻ ion [dp6-GalNAc-2Na]²⁻ (Figure 4A). Subsequent fragmentation (MS³) of this C₅²⁻ ion yielded through glycosidic break a series of the monocharged ions C₂ (m/z 498.0518), C₃ (m/z 696.0432) and C₄ (m/z 1001.0842) (Figure 4B), corresponding to di-, tri- and dp4 respectively, which located the two sulfate groups on the non-reducing part of the dp6 product. Finally, further dissociation by MS⁴ and MS⁵ confirmed the location of the sulfate groups on the GalNAc residue within the central (Z₃⁻ at m/z 300.0375, Figure 4C) and the terminal non-reducing disaccharides (C₂⁻ at m/z 498.0513, Figure 4C, and Z₅^{-0,1}X₆⁻ at m/z 282.0270/312.0374, respectively, Figure 4D) of the disulfated dp6 product. Similar conclusions can be deduced with CS-dp4 analysis (Figure 5). After 24 h incubation, except a major species at m/z 587.6564 (2-) corresponding to the fully unsulfated dp6, a small peak at m/z 632.6847 was detected on mass spectrum, which corresponded to traces of monosulfated dp6 product. Iterative fragmentations from MS² to MS⁶ were

performed to determine the sulfation site along the dp6. Several relevant serial glycosidic bond cleavages were obtained, which allowed the full sequencing: the C₅ ion at m/z 537.0843 and 1075.0843 singly and doubly charged, respectively, (Figure 6) from MS², the C₄ ion at m/z 438.0773 and 899.1452 singly and doubly charged, respectively, (Figure 6) from MS³, the C₃ ion at m/z 336.5373 and 674.0839 singly and doubly charged, respectively, (Figure 6) from MS⁴, and an intense C₂⁻ ion at m/z 498.0575 from MS⁵, evidenced the presence of the sulfate group on the non-reducing end disaccharide unit (Figure 6). MS⁶ of the last disaccharide fragment C₂⁻ yielded the following fragments C₁⁻, Z₅⁻ and ^{0,1}X₆⁻ at m/z 193.0344, m/z 282.0270 and m/z 312.0376, respectively, which unambiguously confirmed that the remaining sulfate to remove is carried by the GalNAc residue at the non-reducing end of the monosulfated dp6 product (Figure 6). The results showed that, same as unsaturated oligosaccharide, the 4-*O*-endosulfatase removed 4-*O*-sulfate groups initially from the reducing end to the non-reducing end of saturated substrates.

Discussion

CS/DS 4-*O*-endosulfatase from *Vibrio* sp. FC509, the first CS/DS sulfatase identified from marine bacteria, was characterized for basic enzymatic properties and substrate-degrading specificity in our previous study (28). The results show that the endosulfatase can specifically remove the 4-*O*-sulfates from 4-*O*-sulfated GalNAc residues in various CS and DS polysaccharide chains, but the desulfation efficiency of the 4-*O*-sulfates is only 17-65%, indicating that there are some structural factors exerting inhibitory effects on the action of this enzyme. Recently, a structural study has shown that the residues at the active site of the 4-*O*-endosulfatase adopt a more favorable conformation to interact with longer CS/DS chains compared with the strict exolytic 4-*O*-sulfatase exoPB4SF (sharing 83% sequence identity with the 4-*O*-endosulfatase), so that hexasaccharides could easily dock into the catalytic pocket of 4-*O*-endosulfatase but not in exoPB4SF (41). However, these structural data do not explain why the 4-*O*-endosulfatase cannot remove all 4-*O*-sulfates from the polysaccharide.

CS/DS hexasaccharide with internal 4-*O*-sulfated disaccharide is the minimal size oligosaccharide to demonstrate the endo-activity of the 4-*O*-endosulfatase. In this study, a series of structure-defined unsaturated hexasaccharides with various sulfation patterns were prepared from the polysaccharide substrates CS-A and CS-E through partial digestion by the endolyase HCLase (35) followed by fractionation using gel filtration and anion-exchange chromatography. Surprisingly, the 4-*O*-endosulfatase can completely remove the 4-*O*-sulfate group of A unit or E unit whatever their location in hexasaccharide (reducing end, non-reducing end, or internal), and this desulfation of A unit or E unit by this enzyme is not inhibited by the adjacent O unit or C unit. However, in the case of octasaccharide ΔC-A-D-C the 4-*O*-sulfate group of the internal A unit could not be removed by this enzyme, suggesting that the D unit connected to A unit should inhibit the action of 4-*O*-endosulfatase. Notably, CS-A from bovine trachea mainly contains A unit, C unit and O unit, but usually no D unit, and only 65% of A units in CS-A were desulfated by the 4-*O*-endosulfatase, indicating that some other structural factors affect the effective action of this enzyme. As mentioned above, our recent study has shown that the binding capacity of the 4-*O*-endosulfatase to long substrate sequences, larger than dp2, plays a key role for its endolytic activity. Accordingly, we found that the hydrolysis of the first 4-*O*-sulfate group on the longer substrate A-A-A is faster than that of equimolar A or A-A, which may due to bigger substrate having a higher probability of

collision with the enzyme. To further investigate the effect of substrate length on the enzymatic activity, a series of size-defined unsaturated oligosaccharides from dp2 to dp12 were prepared from CS-A and used to compare the activity of the 4-*O*-endosulfatase against each of them. The results clearly show that in a short incubation time (10 min) the removal percentage of 4-*O*-sulfates significantly decreases with the increase of substrate size, indicating that the substrate-binding capacity of the enzyme depends on the size of the CS/DS chains. It is likely that removal of the first sulfate groups along the substrate sequence leads to a decrease in substrate affinity, which may explain the low activity of the 4-*O*-endosulfatase against CS-A polysaccharide compared to oligosaccharides.

The 4-*O*-endosulfatase with several GAGs lyases has initially been found in the genome of a marine-derived CS/DS-degrading bacterium *Vibrio* sp. FC509 (28), and thus unsaturated CS/DS oligosaccharides produced by GAGs lyases must be its natural substrates. In our previous study, we have shown that this enzyme prefers to sequentially remove 4-*O*-sulfates from the reducing end of unsaturated dp6 Δ A-A-A. To investigate if the unsaturated double bond of Δ A located at the non-reducing end affects the action direction of the enzyme, we analysed by NanoESI-MSⁿ the action of the enzyme on in this study synthetic saturated hexasaccharide A-A-A, and the results clearly showed that this enzyme also sequentially remove 4-*O*-sulfates from the reducing end to non-reducing end of A-A-A, indicating that Δ A is not a decisive factor to the action direction of the enzyme. However, we found that this enzyme cannot remove 4-*O*-sulfate groups from K unit (GlcUA(3S) β 1-3GalNAc(4S)) and M unit (GlcUA(3S) β 1-3GalNAc(4,6S)), indicating that that 3-*O*-sulfate, unlike 2-*O*-sulfate (30) on GlcUA residue inhibit the hydrolysis of 4-*O*-sulfate from K or M unit.

In conclusion, this study provides a more comprehensive insight into the desulfation pattern of the 4-*O*-endosulfatase from *Vibrio* sp. FC509, which will benefit the application of this enzyme in editing the sulfation patterns of CS/DS oligo-/polysaccharides, as well as their structural and functional studies.

Abbreviations

CS, chondroitin sulfate; DS, dermatan sulfate; GAG, glycosaminoglycan; GlcUA, D-glucuronic acid; IdoUA, L-iduronic acid; HexUA, hexuronic acid; $\Delta^{4,5}$ HexUA, $\Delta^{4,5}$ -unsaturated hexuronic acid; 2S, 4S and 6S, 2-*O*-sulfate, 4-*O*-sulfate and 6-*O*-sulfate, respectively; GalNAc, N-acetyl-D-galactosamine; MS, Mass spectrometry; NMR, Nuclear magnetic resonance; CSase, chondroitinase; 2-AB, 2-aminobenzamide.

Acknowledgement

This work was supported by the National Natural Science Foundation of China (Nos. 31570071, 31971201 and 31800665), the National Natural Science Foundation of Shandong Province (No. ZR2018BC013), the Science and Technology Development Project of Shandong Province (Nos.2018GSF121002), the General Financial Grant from China Postdoctoral Science Foundation Grant (No. 2019M662343), the Major Scientific and Technological Innovation Project (MSTIP) of Shandong Province (2019JZZY010817), and the Project of Taishan Industry Leading Talent of Shandong Province (tscy20160311).

Competing interest

The authors declare that there are no competing interests associated with the manuscript.

Author Contributions

W.W. and X.C. characterized 4-*O*-endosulfatase activity and carried out the oligosaccharide-sequencing experiments. C.P. performed the mass spectrometry experiments, R.J. and L.S. prepared the chondroitin sulfate oligosaccharides. C.L.B. performed the chemical synthesis of the sulfated chondroitin oligosaccharides. K.S. provided the precious oligosaccharides and some important suggestions for the paper preparation. J.L.N. prepared the 4-*O*-endosulfatase, W.W., C.P., R.D. and F.L. have contributed to the analysis of data and to the preparation and edition of the manuscript.

We would like to dedicate this paper to Kazuyuki Sugahara, who unfortunately passed away on July 29, 2020. Kazuyuki played an important role in this research and he is missed very much.

All authors reviewed the results and approved the final version of the manuscript.

References

1. Silbert, J. E., and Sugumaran, G. (2002) Biosynthesis of chondroitin/dermatan sulfate. *IUBMB life* **54**, 177-186 <https://doi.org/10.1080/15216540214923>
2. Maccarana, M., Olander, B., Malmstrom, J., Tiedemann, K., Aebersold, R., Lindahl, U., Li, J. P., and Malmstrom, A. (2006) Biosynthesis of dermatan sulfate: chondroitin-glucuronate C5-epimerase is identical to SART2. *The Journal of biological chemistry* **281**, 11560-11568 <https://doi.org/10.1074/jbc.m513373200>
3. Sugahara, K., Mikami, T., Uyama, T., Mizuguchi, S., Nomura, K., and Kitagawa, H. (2003) Recent advances in the structural biology of chondroitin sulfate and dermatan sulfate. *Curr Opin Struct Biol* **13**, 612-620 <https://doi.org/10.1016/j.sbi.2003.09.011>
4. Izumikawa, T., Kitagawa, H., Mizuguchi, S., Nomura, K. H., Nomura, K., Tamura, J., Gengyo-Ando, K., Mitani, S., and Sugahara, K. (2004) Nematode chondroitin polymerizing factor showing cell-/organ-specific expression is indispensable for chondroitin synthesis and embryonic cell division. *Journal of biological chemistry* **279**, 53755-53761 <https://doi.org/10.1074/jbc.M409615200>
5. Cheng, F., Heinegard, D., Malmstrom, A., Schmidtchen, A., Yoshida, K., and Fransson, L. A. (1994) Patterns of uronosyl epimerization and 4-/6-O-sulphation in chondroitin/dermatan sulphate from decorin and biglycan of various bovine tissues. *Glycobiology* **4**, 685-696 <https://doi.org/10.1093/glycob/4.5.685>
6. Kusche-Gullberg, M., and Kjellen, L. (2003) Sulfotransferases in glycosaminoglycan biosynthesis. *Curr Opin Struct Biol* **13**, 605-611 <https://doi.org/10.1016/j.sbi.2003.08.002>
7. Kluppel, M., Wight, T. N., Chan, C., Hinek, A., and Wrana, J. L. (2005) Maintenance of chondroitin sulfation balance by chondroitin-4-sulfotransferase 1 is required for chondrocyte development and growth factor signaling during cartilage morphogenesis. *Development* **132**, 3989-4003 <https://doi.org/10.1242/dev.01948>
8. Trowbridge, J. M., Rudisill, J. A., Ron, D., and Gallo, R. L. (2002) Dermatan sulfate binds and potentiates activity of keratinocyte growth factor (FGF-7). *The Journal of biological chemistry* **277**, 42815-42820 <https://doi.org/10.1074/jbc.M204959200>
9. Maeda, N., Fukazawa, N., and Hata, T. (2006) The binding of chondroitin sulfate to pleiotrophin/heparin-binding growth-associated molecule is regulated by chain length and oversulfated structures. *Journal of biological chemistry* **281**, 4894-4902 <https://doi.org/10.1074/jbc.M507750200>
10. Faissner, A., Clement, A., Lochter, A., Streit, A., Mandl, C., and Schachner, M. (1994) Isolation of a neural chondroitin sulfate proteoglycan with neurite outgrowth promoting properties. *Journal of cell biology* **126**, 783-799 <https://doi.org/10.1083/jcb.126.3.783>
11. Clement, A. M., Nadanaka, S., Masayama, K., Mandl, C., Sugahara, K., and Faissner, A. (1998) The DSD-1 carbohydrate epitope depends on sulfation, correlates with chondroitin sulfate D motifs, and is sufficient to promote neurite outgrowth. *The Journal of biological chemistry* **273**, 28444-28453 <https://doi.org/10.1074/jbc.273.43.28444>
12. Lafont, F., Rouget, M., Triller, A., Prochiantz, A., and Rousset, A. (1992) In vitro control of neuronal polarity by glycosaminoglycans. *Development* **114**, 17-29
13. Sugahara, K., and Mikami, T. (2007) Chondroitin/dermatan sulfate in the central nervous system. *Curr Opin Struct Biol* **17**, 536-545 <https://doi.org/10.1016/j.sbi.2007.08.01514>. Taylor, K. R., and Gallo, R. L. (2006) Glycosaminoglycans and their proteoglycans: host-associated molecular patterns for initiation and modulation of inflammation. *FASEB journal: official publication of the Federation of American Societies for Experimental Biology* **20**, 9-22 <https://doi.org/10.1096/fj.05-4682rev>

15. Li, F., ten Dam, G. B., Murugan, S., Yamada, S., Hashiguchi, T., Mizumoto, S., Oguri, K., Okayama, M., van Kuppevelt, T. H., and Sugahara, K. (2008) Involvement of Highly Sulfated Chondroitin Sulfate in the Metastasis of the Lewis Lung Carcinoma Cells. *Journal of Biological Chemistry* **283**, 34294-34304 <https://doi.org/10.1074/jbc.M806015200>
16. Mizumoto, S., Takahashi, J., and Sugahara, K. (2012) Receptor for Advanced Glycation End Products (RAGE) Functions as Receptor for Specific Sulfated Glycosaminoglycans, and Anti-RAGE Antibody or Sulfated Glycosaminoglycans Delivered in Vivo Inhibit Pulmonary Metastasis of Tumor Cells. *Journal of Biological Chemistry* **287**, 18985-18994 <https://doi.org/10.1074/jbc.M111.313437>
17. Hsiao, J. C., Chung, C. S., and Chang, W. (1999) Vaccinia virus envelope D8L protein binds to cell surface chondroitin sulfate and mediates the adsorption of intracellular mature virions to cells. *Journal of virology* **73**, 8750-8761 <https://doi.org/10.1016/j.iccn.2004.05.001>
18. Williams, R. K., and Straus, S. E. (1997) Specificity and affinity of binding of herpes simplex virus type 2 glycoprotein B to glycosaminoglycans. *Journal of virology* **71**, 1375-1380 [https://doi.org/10.1016/S0166-0934\(96\)02146-5](https://doi.org/10.1016/S0166-0934(96)02146-5)
19. Bergefall, K., Trybala, E., Johansson, M., Uyama, T., Naito, S., Yamada, S., Kitagawa, H., Sugahara, K., and Bergstrom, T. (2005) Chondroitin sulfate characterized by the E-disaccharide unit is a potent inhibitor of herpes simplex virus infectivity and provides the virus binding sites on gro2C cells. *Journal of Biological Chemistry* **280**, 32193-32199 <https://doi.org/10.1074/jbc.M503645200>
20. Uyama, T., Ishida, M., Izumikawa, T., Trybala, E., Tufaro, F., Bergstrom, T., Sugahara, K., and Kitagawa, H. (2006) Chondroitin 4-O-sulfotransferase-1 regulates E disaccharide expression of chondroitin sulfate required for herpes simplex virus infectivity. *The Journal of biological chemistry* **281**, 38668-38674 <https://doi.org/10.1074/jbc.M609320200>
21. Wang, S., Sugahara, K., and Li, F. (2016) Chondroitin sulfate/dermatan sulfate sulfatases from mammals and bacteria. *Glycoconjugate journal* **33**, 841-851 <https://doi.org/10.1007/s10719-016-9720-0>
22. Hanson, S. R., Best, M. D., and Wong, C. H. (2004) Sulfatases: structure, mechanism, biological activity, inhibition, and synthetic utility. *Angewandte Chemie* **43**, 5736-5763 <https://doi.org/10.1002/anie.200300632>
23. Mikami, T., and Kitagawa, H. (2013) Biosynthesis and function of chondroitin sulfate. *Biochimica et biophysica acta* **1830**, 4719-4733 <https://doi.org/10.1016/j.bbagen.2013.06.006>
24. Bhattacharyya, S., Kotlo, K., Shukla, S., Danziger, R. S., and Tobacman, J. K. (2008) Distinct effects of N-acetylgalactosamine-4-sulfatase and galactose-6-sulfatase expression on chondroitin sulfates. *The Journal of biological chemistry* **283**, 9523-9530 <https://doi.org/10.1074/jbc.M707967200>
25. Myette, J. R., Shriver, Z., Claycamp, C., McLean, M. W., Venkataraman, G., and Sasisekharan, R. (2003) The heparin/heparan sulfate 2-O-sulfatase from *Flavobacterium heparinum*. Molecular cloning, recombinant expression, and biochemical characterization. *The Journal of biological chemistry* **278**, 12157-12166 <https://doi.org/10.1074/jbc.M211420200>
26. Sugahara, K., and Kojima, T. (1996) Specificity studies of bacterial sulfatases by means of structurally defined sulfated oligosaccharides isolated from shark cartilage chondroitin sulfate D. *European journal of biochemistry* **239**, 865-870 <https://doi.org/10.1111/j.1432-1033.1996.0865u.x>
27. Ulmer, J. E., Vilen, E. M., Namburi, R. B., Benjdia, A., Beneteau, J., Malleron, A., Bonnaffe, D., Driguez, P. A., Descroix, K., Lassalle, G., Le Narvor, C., Sandstrom, C., Spillmann, D., and Berteau, O. (2014) Characterization of glycosaminoglycan (GAG) sulfatases from the human gut symbiont *Bacteroides thetaiotaomicron* reveals the first GAG-specific bacterial endosulfatase. *The Journal of*

- biological chemistry* **289**, 24289-24303 <https://doi.org/10.1074/jbc.M114.573303>
28. Wang, W., Han, W., Cai, X., Zheng, X., Sugahara, K., and Li, F. (2015) Cloning and Characterization of a Novel Chondroitin Sulfate/Dermatan Sulfate 4-O-Endosulfatase from a Marine Bacterium. *Journal of Biological Chemistry* **290**, 7823-7832 <https://doi.org/10.1074/jbc.M114.629154>
 29. Wang, W., Cai, X., Han, N., Han, W., Sugahara, K., and Li, F. (2017) Sequencing of chondroitin sulfate oligosaccharides using a novel exolyase from a marine bacterium that degrades hyaluronan and chondroitin sulfate/dermatan sulfate. *Biochemical Journal* **474**, 3831-3848 <https://doi.org/10.1042/BCJ20170591>
 30. Han, W., Wang, W., Zhao, M., Sugahara, K., and Li, F. (2014) A Novel Eliminase from a Marine Bacterium That Degrades Hyaluronan and Chondroitin Sulfate. *Journal of Biological Chemistry* **289**, 27886-27898 <https://doi.org/10.1074/jbc.M114.590752>
 31. Pothacharoen, P., Kalayanamitra, K., Deepa, S. S., Fukui, S., Hattori, T., Fukushima, N., Hardingham, T., Kongtawelert, P., and Sugahara, K. (2007) Two related but distinct chondroitin sulfate mimetope octasaccharide sequences recognized by monoclonal antibody WF6. *Journal of biological chemistry* **282**, 35232-35246 <https://doi.org/10.1074/jbc.M702255200>
 32. Jacquinet, J. C., Lopin-Bon, C., and Vibert, A. (2009) From polymer to size-defined oligomers: a highly divergent and stereocontrolled construction of chondroitin sulfate A, C, D, E, K, L, and M oligomers from a single precursor: part 2. *Chemistry (Weinheim an der Bergstrasse, Germany)* **15**, 9579-9595 <https://doi.org/10.1002/chem.200900741>
 33. Yamagata, T., Saito, H., Habuchi, O., and Suzuki, S. (1968) Purification and properties of bacterial chondroitinases and chondrosulfatases. *The Journal of biological chemistry* **243**, 1523-1535 [https://doi.org/10.1016/0003-2697\(68\)90101-2](https://doi.org/10.1016/0003-2697(68)90101-2)
 34. Li, F., Nandini, C. D., Hattori, T., Bao, X., Murayama, D., Nakamura, T., Fukushima, N., and Sugahara, K. (2010) Structure of pleiotrophin- and hepatocyte growth factor-binding sulfated hexasaccharide determined by biochemical and computational approaches. *The Journal of biological chemistry* **285**, 27673-27685 <https://doi.org/10.1074/jbc.M110.118703>
 35. Bigge, J. C., Patel, T. P., Bruce, J. A., Goulding, P. N., Charles, S. M., and Parekh, R. B. (1995) Nonselective and efficient fluorescent labeling of glycans using 2-amino benzamide and anthranilic acid. *Analytical biochemistry* **230**, 229-238 <https://doi.org/10.1006/abio.1995.1468>
 36. Bodet, P. E., Salard, I., Przybylski, C., Gonnet, F., Gomila, C., Ausseil, J., and Daniel, R. (2017) Efficient recovery of glycosaminoglycan oligosaccharides from polyacrylamide gel electrophoresis combined with mass spectrometry analysis. *Analytical and bioanalytical chemistry* **409**, 1257-1269 <https://doi.org/10.1007/s00216-016-0052-5>
 37. Przybylski, C., Gonnet, F., Bonnaffe, D., Hersant, Y., Lortat-Jacob, H., and Daniel, R. (2010) HABA-based ionic liquid matrices for UV-MALDI-MS analysis of heparin and heparan sulfate oligosaccharides. *Glycobiology* **20**, 224-234 <https://doi.org/10.1093/glycob/cwp169>
 38. Domon, B., and Costello, C. E. (1988) A systematic nomenclature for carbohydrate fragmentations in FAB-MS/MS spectra of glycoconjugates. *Glycoconjugate journal* **5**, 397-409 <https://doi.org/10.1007/BF01049915>
 39. Kinoshita, A., and Sugahara, K. (1999) Microanalysis of glycosaminoglycan-derived oligosaccharides labeled with a fluorophore 2-aminobenzamide by high-performance liquid chromatography: application to disaccharide composition analysis and exosequencing of oligosaccharides. *Analytical biochemistry* **269**, 367-378 <https://doi.org/10.1006/abio.1999.4027>
 40. Sugahara, K., and Yamada, S. (2000) Structure and Function of Oversulfated Chondroitin Sulfate

- Variants. *Trends in Glycoscience and Glycotechnology* **12**, 321-349 <https://doi.org/10.4052/tigg.12.321>
41. Wang, S., Su, T., Zhang, Q., Guan, J., He, J., Gu, L., and Li, F. (2019) Comparative Study of Two Chondroitin Sulfate/Dermatan Sulfate 4-O-Sulfatases With High Identity. *Front Microbiol* **10**, 1309 <https://doi.org/10.3389/fmicb.2019.01309>
 42. Morimoto-Tomita, M., Uchimura, K., Werb, Z., Hemmerich, S., and Rosen, S. D. (2002) Cloning and characterization of two extracellular heparin-degrading endosulfatases in mice and humans. *The Journal of biological chemistry* **277**, 49175-49185 <https://doi.org/10.1074/jbc.M205131200>

Table 1. Disaccharide composition of dp6s fractions isolated from CS-A and CS-E. Numbers in parentheses indicate the percentage recoveries, which were calculated based upon the peak area on an HPLC chromatogram and are expressed relative to the amount of each parent dp6 fraction used for degradation.

Fraction	Disaccharide formed
CS-A3	$\Delta^{4,5}\text{HexUA}\alpha\text{1-3GalNAc}$ (106%)
	$\Delta^{4,5}\text{HexUA}\alpha\text{1-3GalNAc(4S)}$ (101%)
	$\Delta^{4,5}\text{HexUA}\alpha\text{1-3GalNAc(6S)}$ (98%)
CS-A4	$\Delta^{4,5}\text{HexUA}\alpha\text{1-3GalNAc}$ (112%)
	$\Delta^{4,5}\text{HexUA}\alpha\text{1-3GalNAc(4S)}$ (207%)
CS-A5	$\Delta^{4,5}\text{HexUA}\alpha\text{1-3GalNAc}$ (110%)
	$\Delta^{4,5}\text{HexUA}\alpha\text{1-3GalNAc(4S)}$ (202%)
CS-A7	$\Delta^{4,5}\text{HexUA}\alpha\text{1-3GalNAc(6S)}$ (302%)
CS-A9	$\Delta^{4,5}\text{HexUA}\alpha\text{1-3GalNAc(4S)}$ (110%)
	$\Delta^{4,5}\text{HexUA}\alpha\text{1-3GalNAc(6S)}$ (223%)
CS-A10-1	$\Delta^{4,5}\text{HexUA}\alpha\text{1-3GalNAc(4S)}$ (198%)
	$\Delta^{4,5}\text{HexUA}\alpha\text{1-3GalNAc(6S)}$ (102%)
CS-A10-2	$\Delta^{4,5}\text{HexUA}\alpha\text{1-3GalNAc(4S)}$ (99%)
	$\Delta^{4,5}\text{HexUA}\alpha\text{1-3GalNAc(6S)}$ (187%)
CS-A10-3	$\Delta^{4,5}\text{HexUA}\alpha\text{1-3GalNAc(4S)}$ (105%)
	$\Delta^{4,5}\text{HexUA}\alpha\text{1-3GalNAc(6S)}$ (192%)
CS-A11	$\Delta^{4,5}\text{HexUA}\alpha\text{1-3GalNAc(4S)}$ (298%)
CS-E7	$\Delta^{4,5}\text{HexUA}\alpha\text{1-3GalNAc(6S)}$ (97%)
	$\Delta^{4,5}\text{HexUA}\alpha\text{1-3GalNAc(4S)}$ (102%)
	$\Delta^{4,5}\text{HexUA}\alpha\text{1-3GalNAc(4S,6S)}$ (101%)
CS-E9	$\Delta^{4,5}\text{HexUA}\alpha\text{1-3GalNAc(4S)}$ (197%)
	$\Delta^{4,5}\text{HexUA}\alpha\text{1-3GalNAc(4S,6S)}$ (103%)
CS-E13	$\Delta^{4,5}\text{HexUA}\alpha\text{1-3GalNAc(6S)}$ (102%)
	$\Delta^{4,5}\text{HexUA}\alpha\text{1-3GalNAc(4S,6S)}$ (201%)
CS-E15	$\Delta^{4,5}\text{HexUA}\alpha\text{1-3GalNAc(4S)}$ (99%)
	$\Delta^{4,5}\text{HexUA}\alpha\text{1-3GalNAc(4S,6S)}$ (200%)

Table 2. Sugar composition and structure of the dp6s fractions.

Values are expressed relative to the dp6s values, which were determined by absorption at 232 nm.

Fraction	Yield/ nmol	Sequencing of dp6s
CS-A3	8.523	$\Delta^{4,5}\text{HexUA}\alpha\text{1-3GalNAc(6S)}\beta\text{1-4GlcUA}\beta\text{1-3GalNAc}\beta\text{1-4GlcUA}\beta\text{1-3GalNAc(4S)}$
CS-A4	4.867	$\Delta^{4,5}\text{HexUA}\alpha\text{1-3GalNAc}\beta\text{1-4GlcUA}\beta\text{1-3GalNAc(4S)}\beta\text{1-4GlcUA}\beta\text{1-3GalNAc(4S)}$
CS-A5	19.957	$\Delta^{4,5}\text{HexUA}\alpha\text{1-3GalNAc(4S)}\beta\text{1-4GlcUA}\beta\text{1-3GalNAc}\beta\text{1-4GlcUA}\beta\text{1-3GalNAc(4S)}$
CS-A7	10.063	$\Delta^{4,5}\text{HexUA}\alpha\text{1-3GalNAc(6S)}\beta\text{1-4GlcUA}\beta\text{1-3GalNAc(6S)}\beta\text{1-4GlcUA}\beta\text{1-3GalNAc(6S)}$
CS-A9	18.378	$\Delta^{4,5}\text{HexUA}\alpha\text{1-3GalNAc(4S)}\beta\text{1-4GlcUA}\beta\text{1-3GalNAc(6S)}\beta\text{1-4GlcUA}\beta\text{1-3GalNAc(6S)}$
CS-A10-1	15.816	$\Delta^{4,5}\text{HexUA}\alpha\text{1-3GalNAc(4S)}\beta\text{1-4GlcUA}\beta\text{1-3GalNAc(4S)}\beta\text{1-4GlcUA}\beta\text{1-3GalNAc(6S)}$
CS-A10-2	3.181	$\Delta^{4,5}\text{HexUA}\alpha\text{1-3GalNAc(6S)}\beta\text{1-4GlcUA}\beta\text{1-3GalNAc(4S)}\beta\text{1-4GlcUA}\beta\text{1-3GalNAc(6S)}$
CS-A10-3	3.052	$\Delta^{4,5}\text{HexUA}\alpha\text{1-3GalNAc(6S)}\beta\text{1-4GlcUA}\beta\text{1-3GalNAc(6S)}\beta\text{1-4GlcUA}\beta\text{1-3GalNAc(4S)}$
CS-A11	267.995	$\Delta^{4,5}\text{HexUA}\alpha\text{1-3GalNAc(4S)}\beta\text{1-4GlcUA}\beta\text{1-3GalNAc(4S)}\beta\text{1-4GlcUA}\beta\text{1-3GalNAc(4S)}$
CS-E7	15.756	$\Delta^{4,5}\text{HexUA}\alpha\text{1-3GalNAc(4S,6S)}\beta\text{1-4GlcUA}\beta\text{1-3GalNAc(4S)}\beta\text{1-4GlcUA}\beta\text{1-3GalNAc(6S)}$
CS-E9	28.507	$\Delta^{4,5}\text{HexUA}\alpha\text{1-3GalNAc(4S,6S)}\beta\text{1-4GlcUA}\beta\text{1-3GalNAc(4S)}\beta\text{1-4GlcUA}\beta\text{1-3GalNAc(4S)}$
CS-E13	6.033	$\Delta^{4,5}\text{HexUA}\alpha\text{1-3GalNAc(4S,6S)}\beta\text{1-4GlcUA}\beta\text{1-3GalNAc(4S,6S)}\beta\text{1-4GlcUA}\beta\text{1-3GalNAc(6S)}$
CS-E15	6.285	$\Delta^{4,5}\text{HexUA}\alpha\text{1-3GalNAc(4S,6S)}\beta\text{1-4GlcUA}\beta\text{1-3GalNAc(4S,6S)}\beta\text{1-4GlcUA}\beta\text{1-3GalNAc(4S)}$

Table 3. Structure comparison of oligosaccharides before and after treated with 4-*O*-endosulfatase. Consistent with results obtained from disaccharide composition of sulfatase-treated oligosaccharides, we determined the structural sequence of the degradation products.

Fraction	Sequencing of oligosaccharides	Sequencing of sulfatase-treated oligosaccharides
CS-A3	Δ C-O-A	Δ C-O-O
CS-A4	Δ O-A-A	Δ O-O-O
CS-A5	Δ A-O-A	Δ O-O-O
CS-A7	Δ C-C-C	Δ C-C-C
CS-A9	Δ A-C-C	Δ O-C-C
CS-A10-1	Δ A-A-C	Δ O-O-C
CS-A10-2	Δ C-A-C	Δ C-O-C
CS-A10-3	Δ C-C-A	Δ C-C-O
CS-A11	Δ A-A-A	Δ O-O-O
CS-E7	Δ E-A-C	Δ C-O-C
CS-E9	Δ E-A-A	Δ C-O-O
CS-E13	Δ E-E-C	Δ C-C-C
CS-E15	Δ E-E-A	Δ C-C-O
Octasaccharide	Δ C-A-D-C	Δ C-A-D-C

Table 4. The percentage of 4-O-sulfate removed from CS-A oligosaccharide

The sulfate content was determined at the disaccharide level after incubation of oligosaccharides with the 4-*O*-sulfatase as described in *Experimental Procedures*. 100% refers to the level content in control incubation without 4-*O*-sulfatase.

oligosaccharide	4-O-sulfate removed percentage (%)
Disaccharide (DP2)	95.6
Tetrasaccharide (DP4)	81.4
Hexasaccharide (DP6)	70.8
Octasaccharide (DP8)	65.2
Decasaccharide (DP10)	50.2
Dodecasaccharide (DP12)	31.3

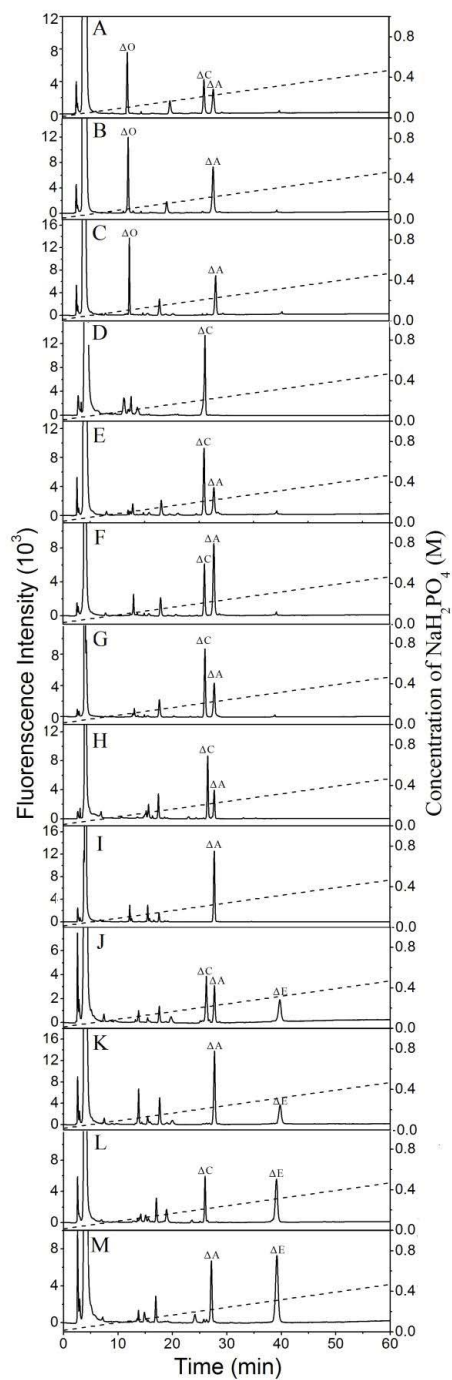


FIGURE 1. Disaccharide composition of dp6s fractions. The dp6s fractions of CS-A3(A), CS-A4(B), CS-A5(C), CS-A7(D), CS-A9(E), CS-A10-1(F), CS-A10-2(G), CS-A10-3(H), CS-A11(I), CS-E7(J), CS-E9(K), CS-E13(L) and CS-E15(M) were degraded with CSase ABC, labeled with 2-AB, and then analyzed by anion exchange HPLC as described in experimental procedures. The elution positions of the following standard disaccharides are indicated: ΔO , $\Delta^{4,5}\text{HexUA}\alpha 1\text{-3GalNAc}$; ΔC , $\Delta^{4,5}\text{HexUA}\alpha 1\text{-3GalNAc(6S)}$; ΔA : $\Delta^{4,5}\text{HexUA}\alpha 1\text{-3GalNAc(4S)}$; ΔE : $\Delta^{4,5}\text{HexUA}\alpha 1\text{-3GalNAc(4S,6S)}$.

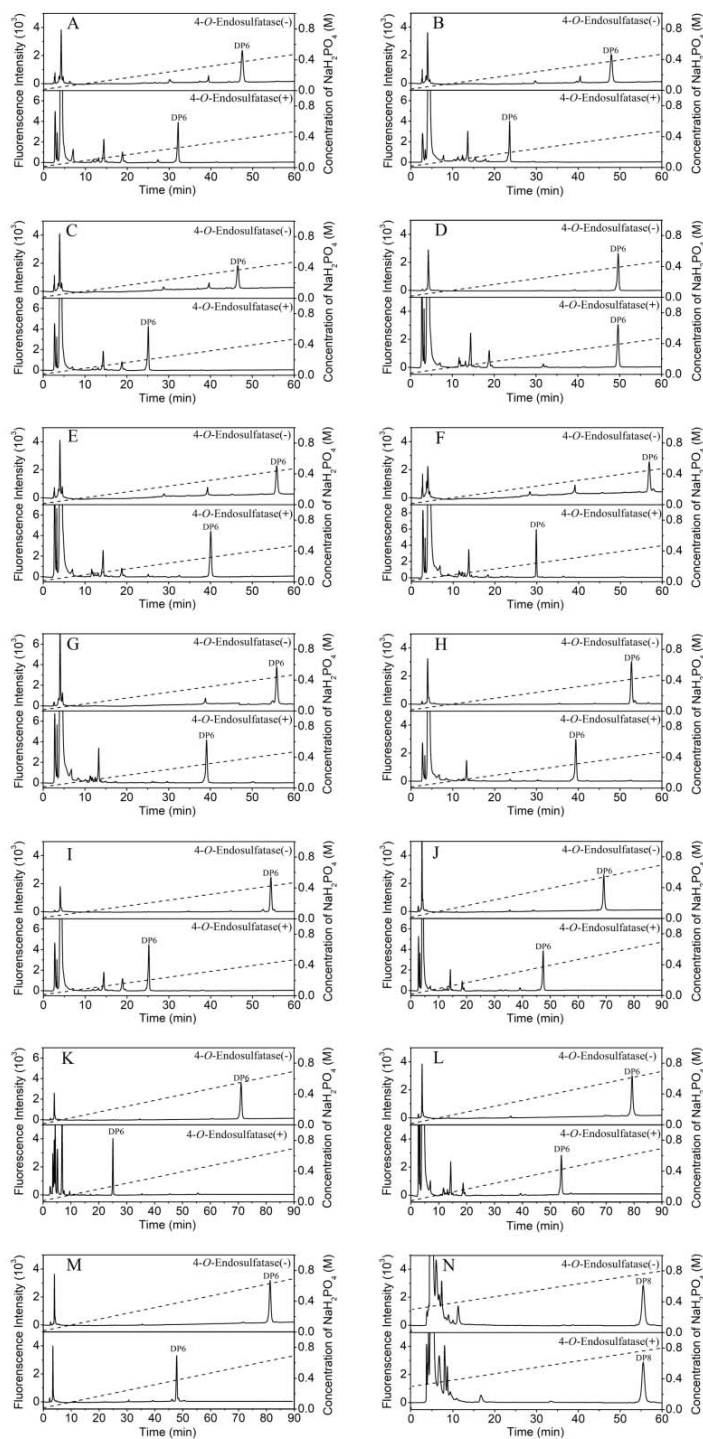


FIGURE 2. Analysis of the final products of CS/DS oligosaccharides digested with 4-O-endosulfatase. Unsaturated CS/DS oligosaccharides of CS-A3 (A), CS-A4 (B), CS-A5 (C), CS-A7 (D), CS-A9 (E), CS-A10-1 (F), CS-A10-2 (G), CS-A10-3 (H), CS-A11(I), CS-E7 (J), CS-E9 (K), CS-E13 (L), CS-E15 (M) and octasaccharide (N) were exhaustively digested without (top) or with (bottom) 4-O-endosulfatase, labeled with 2-AB, and then analyzed by anion exchange HPLC as described under “Experimental Procedures.”

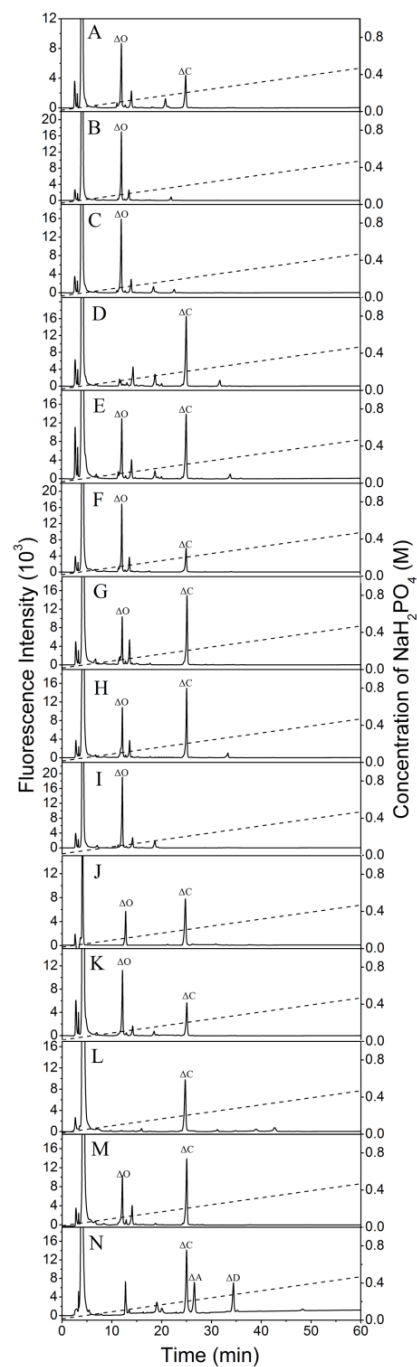


FIGURE 3 Disaccharide composition analysis of oligosaccharides digested with 4-O-endosulfatase. Dp6s of CS-A3 (A), CS-A4 (B), CS-A5 (C), CS-A7 (D), CS-A9 (E), CS-A10-1 (F), CS-A10-2 (G), CS-A10-3 (H), CS-A11 (I), CS-E7 (J), CS-E9 (K), CS-E13 (L), CS-E15 (M) and octasaccharide (N) were exhaustively digested with 4-O-endosulfatase and then further digested with CSase ABC, the products were analyzed by anion exchange HPLC as described under “Experimental Procedures.” The elution positions of the following standard disaccharides are indicated: ΔO , $\Delta^{4,5}\text{HexUA}\alpha 1\text{-3GalNAc}$; ΔC , $\Delta^{4,5}\text{HexUA}\alpha 1\text{-3GalNAc(6S)}$; ΔA : $\Delta^{4,5}\text{HexUA}\alpha 1\text{-3GalNAc(4S)}$; ΔD : $\Delta^{4,5}\text{HexUA(2S)}\alpha 1\text{-3GalNAc(6S)}$.

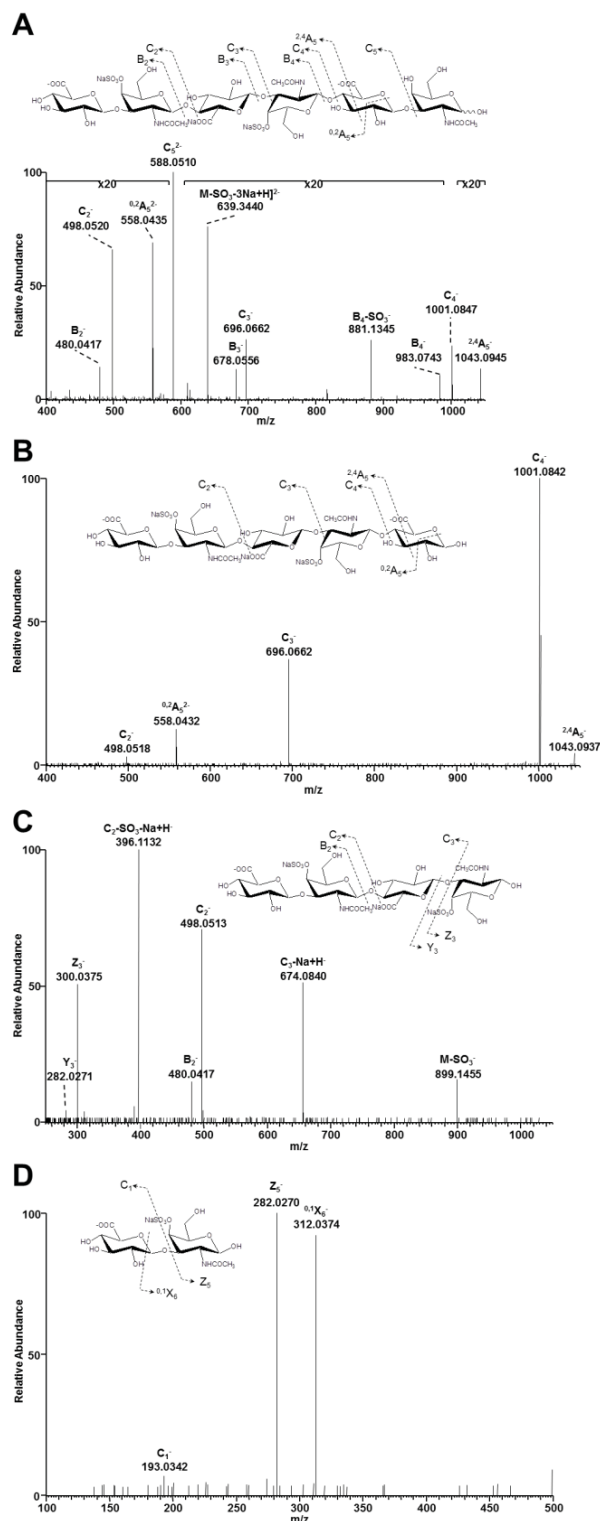


Figure 4. Negative nanoESI sequential fragmentations of the synthetic A-A-A ion at m/z 689.5937 after sulfatase action during 3 h. (A) MS^2 spectrum of the $[dp6-SO_3-3Na+H]^{2-}$ precursor ion at m/z 689.5937, (B) MS^3 spectrum of the C_5^{2-} ion at m/z 588.0510, (C) MS^4 spectrum of the C_4^- ion at m/z 1001.0842 and (D) MS^5 spectrum of the C_2^- ion at m/z 498.0513.

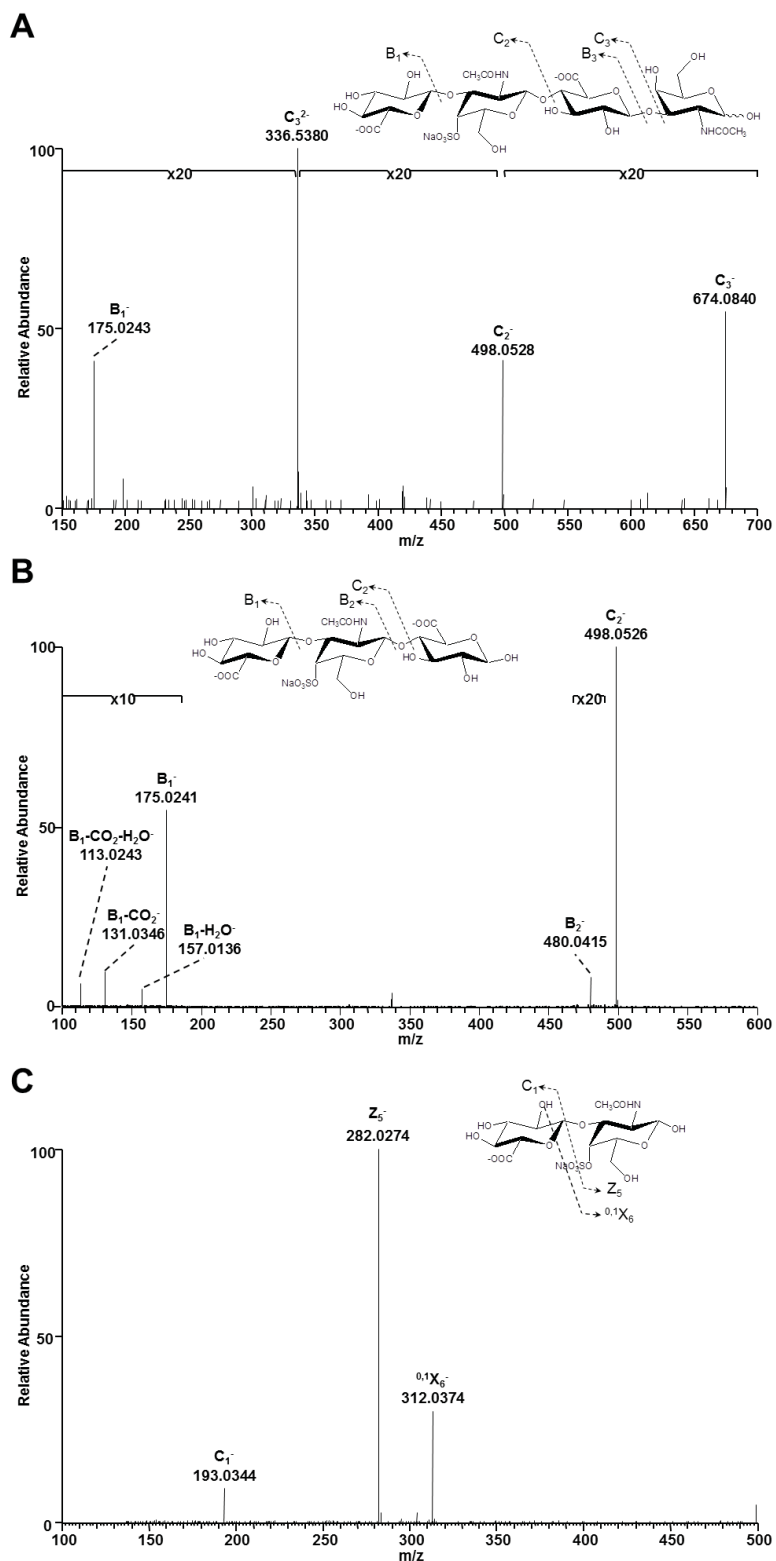


Figure 5. Negative nanoESI sequential fragmentations of the synthetic A-A ion at m/z 438.0777 after sulfatase action during 3 h. (A) MS² spectrum of the $[dp4 -SO_3+3Na+H]^{2-}$ precursor ion at m/z 438.0777, (B) MS³ spectrum of the C_3^{2-} ion at m/z 336.5380 and (C) MS⁴ spectrum of the C_2^- ion at m/z 498.0528.

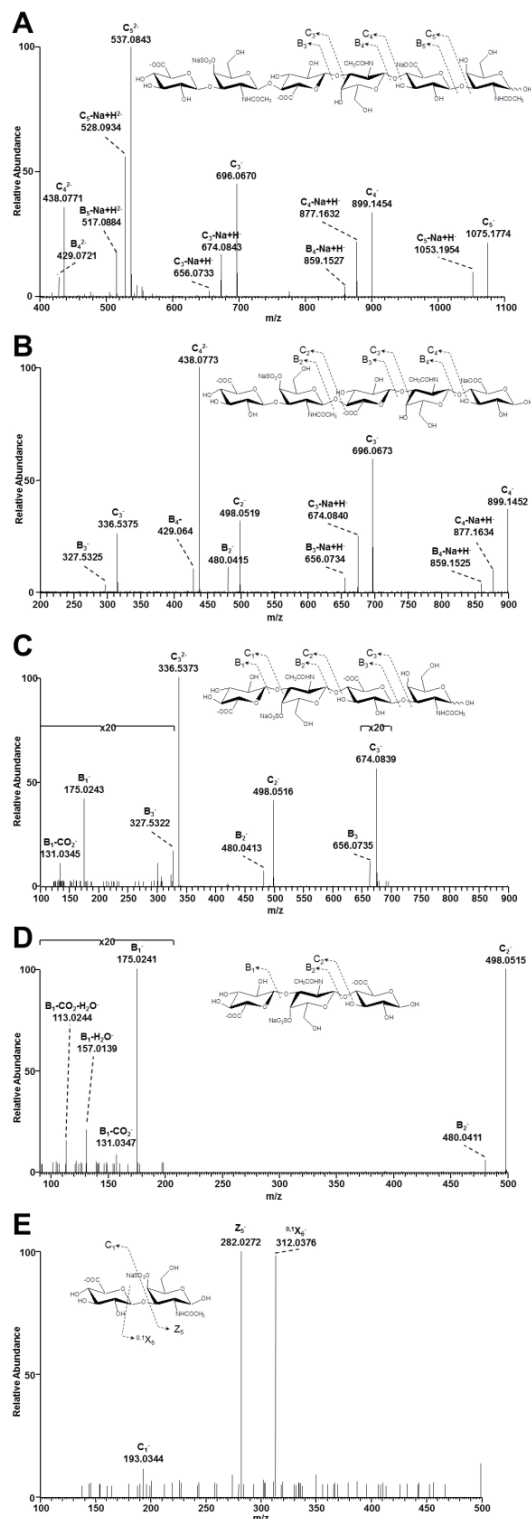


Figure 6. Negative nanoESI sequential fragmentations of the synthetic A-A-A ion at m/z 632.6847 after sulfatase action during 24 h. (A) MS^2 spectrum of the $[dp6-2SO_3-4Na+2H]^{2-}$ precursor ion at m/z 632.6847, (B) MS^3 spectrum of the C_5^{2-} ion at m/z 537.0843, (C) MS^4 spectrum of the C_4^{2-} ion at m/z 438.0773, (D) MS^5 spectrum of the C_3^- ion at m/z 336.5373 and (E) MS^6 spectrum of the C_2^- ion at m/z 498.0515.